RSC Advances

ROYAL SOCIETY OF CHEMISTRY

www.rsc.org/advances

Journal Name

RSCPublishing

ARTICLE

Chemical Colorimetric Square Wave and its Derived Logic Gates Based on Tunable Growth of Plasmonic Gold Nanoparticles

ite this: DOI: 10.1039/x0xx00000x

Received 00th January 2012,
Accepted 00th January 2012

DOI: 10.1039/x0xx00000x

www.rsc.org/

Yanjuan Zhou, Kaiyu He, Shengquan Liu, Yong Li, Zhou Nie*, Yan Huang, Shouzhuo Yao

Plasmonic change in the growth process of gold nanoparticles (AuNPs) is not only intriguing for material science, but also promising for developing new colorimetric biosensors and logic devices. Herein, we report a novel AuNPs-based plasmonic phenomenon, namely chemical colorimetric square wave (CCSW) and further develop a series of label-free and simple colorimetric logic gates based on the CCSW. The CCSW refers to the unique phenomenon of silver ion concentration or pH-dependent discontinuous colorimetric signal change (blue-red-blue) observed in hydrogen peroxide-mediated AuNPs generation process. By setting blue and red color as OFF and ON colorimetric signal, respectively, the colorimetric signal profile of CCSW can be outputted in a format of OFF-ON-OFF, presenting an analog of electronic square wave. Thereby, two CCSWs were successfully constructed, namely Ag^{+}-CCSW and pH-CCSW. Subsequently, colorimetric AND, INHIBIT and OR logic gates were built via rational integrations of two CCSWs. Unlike traditional AuNPs-based logic gates with target-triggered AuNPs crosslinking, these CCSW-based logic gates relied on the controllable growth of AuNPs, which are facile, fast and cost-efficient, avoiding tedious modification of AuNPs probe and complicated operations. Therefore, our proposed CCSW and its derived logic gates present a promising application of plasmonic noble metal nanomaterials.

1. Introduction

Noble metal nanoparticles are excellent candidates as plasmonic building blocks because of their chemical inertness and ability of supporting plasmon resonances in the visible or the near infrared region[1, 2]. As typical example of noble metal nanoparticles, AuNPs have been widely used in biosensing[3], biomedicine[4], biodiagnosis[5] and molecular logic gates[6] due to the unique and tunable properties, including surface plasmon resonances (SPR), local surface plasmon resonances (LSPR), biocompatibility and facile surface modification. In general, the dispersion or aggregation of AuNPs by modulating the distance between nanoparticles through crosslinking[7-10] and non-crosslinking[11-14] would cause the shift of plasmon band and combination of plasmons, which results in distinct color change of AuNPs solutions. Therefore, based on this intriguing phenomenon, numerous efforts have been made to develop AuNPs colorimetric biosensors relied on the controllable aggregation of AuNPs for detection of metal ions[13, 15], small molecules[11, 16], nucleic acids[17, 18], proteins[19-21] and even cells[22, 23]. The pre-synthesized AuNPs are exploited in these AuNPs-based plasmonic biosensors for target-triggered aggregation. Currently, the plasmonic changes during synthesis or generation process of nanoparticles have emerged as a new alternative mechanism to develop plasmonic biosensor. For example, Molly's group developed plasmonic ELISA via colorimetric read-out of AuNPs generation to realize sensitive detection of the cancer biomarker prostate specific antigen and HIV-1 capsid antigen p24[24]. Furthermore, they reported an ultra-sensitive immunoassay to detect prostate specific antigen based on the enzyme-guided growth of silver nano-crystal on plasmonic gold nanostars[25]. In addition, our group developed a simple colorimetric assay for blood glucose dependent on enzymatically modulated generation of gold nanorods (AuNRs)[26]. The application of plasmonic change during noble metal nanoparticles generation is still in an early stage, which provokes further efforts to develop their applications in broader fields.

In order to develop the computing system alternative to silicon-based computer, there is an increasing interest in studying molecules or nanomaterials-based devices in which output states (0 or 1) depend on input conditions (0/0, 1/0, 0/1, or 1/1)[27]. Many biomolecules and nano-materials have been applied to construct various logic gates (*e.g.* AND, OR, XOR and INHIBIT logic gate)[28, 29], and these moleculars and nanoscale computing systems hold great promise for applications in computer and life science. Recently, colorimetric logic gate is particularly attractive for point-of-use applications due to its low cost, rapidness, and especial ease of readout (even with naked eyes)[30]. AuNPs was employed as ideal candidates for colorimetric logic gate due to the extremely high extinction coefficients and the strongly distance-dependent optical properties[31]. The outputs of AuNPs-based logic gates can be visually distinguished by color changes and easily monitored via UV-Vis absorption spectra[32, 33]. For example, Jiang's group reported resettable, multi-readout logic gates based on controllably reversible

aggregation of AuNPs[34]. Yang's group reported colorimetric logic gates for small molecules using split/integrated aptamers and unmodified AuNPs[35]. Most of previously reported cases of AuNPs-based logic gates are dependent on the AuNPs aggregation-caused color change and pre-synthesized AuNPs. However, the colorimetric logic gates based on the plasmonic changes during generation process of AuNPs are scarce.

Herein, we report a novel AuNPs-based plasmonic phenomenon, namely chemical colorimetric square wave (CCSW), and further develop a series of label-free and simple colorimetric logic gates based on the CCSW. We investigated the hydrogen peroxide (H_2O_2)-mediated AuNPs synthesis and found an interesting discontinuous colorimetric signal change (blue to red and then return to blue, blue-red-blue) with increasing concentration of additive silver ion (Ag^+) or pH value. If the red solution is defined as colorimetric signal ON and the blue one as OFF, this Ag^+ concentration or pH dependent colorimetric signal change shows an OFF-ON-OFF profile with two distinct signal switches, one for signal on and the other for signal off, which is analogous to square wave pulse in electronics, therefore we named this three-stage profile as colorimetric chemical square wave (CCSW). Hence, we successfully constructed Ag^+ concentration dependent CCSW (Ag^+-CCSW) and pH dependent CCSW (pH-CCSW) based on the regulation of Ag^+ concentration and pH on AuNPs preparation, respectively. In addition, we built colorimetric AND, INHIBIT and OR logic gates via rational integrations of two CCSWs. These logic gates are facile, fast and cost-efficient, which tremendously avoided the tedious modification process to prepare AuNPs probe and the complicated operations in common AuNPs crosslinking-based logic gates. We present an instance of nanoscale logic gates based on AuNPs generation-induced plsmonic change, which expands the application of colorimetric logic gates.

2. Experimental details

2.1 Materials

Gold (III) chloride trihydrate ($HAuCl_4 \cdot 3H_2O$) was purchased from Sigma-Aldrich (St. Louis, USA). 30% (v/v) H_2O_2 was supplied by Sinopharm Chemical Reagent Inc. (Shanghai, China). All chemical reagents were of analytical grade and used without further purification. Ultra-pure water (18.25 MΩ · cm) was prepared from a Millipore system and used in all experiments.

2.2 Synthesis of AuNPs

H_2O_2 solutions with different concentrations in 2-(N-morpholino) ethanesulphonic acid buffer (MES buffer) (1 mM, pH 6.5) were loaded with 96-well microtiter plate. Then $HAuCl_4$ (0.1 mM) was added to each well of the plate, stirred, and then incubated at 37°C. Both the absorbance of 550 nm and photographs were recorded at 15 min after the addition of gold precursor. Experiments performed with different concentrations of H_2O_2 were carried out in the same method except for using a series of concentrations of H_2O_2 (0 ~ 180 μM) to confirm the critical concentration of H_2O_2. To investigate the effect of Ag^+ on H_2O_2-mediated AuNPs generation, the AuNPs synthesis was carried out in the same process except adding $AgNO_3$ (0 ~ 5 μM) before the addition of H_2O_2. To evaluate the effect of pH on H_2O_2-mediated AuNPs generation, the AuNPs synthesis was carried out in the same process except using a series of MES buffer with different pH values (3.2 ~ 8.5).

2.3 Characterizations

UV-Vis spectra of the resulting solutions were recorded by SynergyTM Mx Multi-Mode Microplate Reader (BioTek, USA). The nanostructures and morphologies were investigated by a JEOL JEC 3010 transmission electron microscopic (TEM). The energy dispersive X-ray spectroscopy (EDX) analysis were performed at 200 kV. Dynamic light scattering (DLS) was used to measure hydrodynamic size by Zetasizer Nano ZS90.

3. Results and discussions

3.1 Preparation of AuNPs using H_2O_2

A number of successful methods have been developed to synthesize AuNPs with different sizes and shapes in aqueous and organic media, such as citrate reduction[36] and the Brust-Schiffrin method[37]. Recently, synthesis of AuNPs by reduction of $HAuCl_4$ with H_2O_2 has been reported[24]. This method is fairly simple, fast and environmentally friendly, and the size and morphology of AuNPs prepared by this method is especially sensitive towards the concentration change of H_2O_2. At first, we exploited H_2O_2 to reduce $HAuCl_4$ and investigated the effect of H_2O_2 concentration on the color changes of the AuNPs obtained. As shown in Figure 1A, the color of AuNPs solutions had an obvious change from purple to red in a narrow concentration range of H_2O_2 from 60 μM to 80 μM, which was similar to the results reported in the literature[24]. Accordingly, as shown in Figure S1A, the AuNPs solutions with H_2O_2 more than 80 μM shows the identical absorption spectra with maximum absorbance at 550 nm, whereas the absorption peaks of AuNPs samples gradually broaden and red-shift with remarkable diminished absorbance when H_2O_2 concentration drops below 80 μM. The final states and morphology of AuNPs solutions have been further characterized by transmission electron microscopic (TEM) and dynamic light scattering (DLS). TEM image exhibited that the AuNPs are aggregated in clusters comprising a large number of particles with a diameter of 35 ± 10 nm (Figure S2A) at low concentration of H_2O_2 (60 μM). Conversely, well-dispersed AuNPs with an average diameter of 34 ± 4 nm were formed in the presence of 80 μM H_2O_2 (Figure S2B). The DLS results (Figure S3) implied that the AuNPs grown upon 80 μM H_2O_2 have a smaller size and narrower size distribution in comparison with those grown upon 60 μM H_2O_2. The ratio of A_{550} and A_{650} was used to represent the colorimetric signal of nanoparticles in all experiments[38]. The dynamic measurement (Figure S1B) of AuNPs growth indicates that H_2O_2 concentration above 80 μM all causes quick colorimetric signal change to the final $A_{550/650}$ value greater than 2 in 10 min, indicating fast growth of AuNPs by reduction of H_2O_2. Oppositely, H_2O_2 concentration below 80 μM led to small or negligible change of colorimetric signal in 15 min and final $A_{550/650}$ values are less than 2.

3.2 Establishment of the Ag^+-CCSW based on Ag^+-mediated AuNPs growth

Silver ion has been widely used to assist the growth of AuNPs in the seed-mediated approaches[39]. Our above-mentioned results demonstrated that the formation of AuNPs was correlated with the concentration of H_2O_2, and well-dispersed AuNPs cannot be obtained at 60 μM H_2O_2. Hence, we speculate that Ag^+ might be applied to assist the formation of well-dispersed AuNPs under the condition of 60 μM H_2O_2 (Figure 1B). Fortunately, as we expected, an intriguing phenomenon was observed upon Ag^+ addition. As shown in Figure 1C, red AuNPs dispersion was obtained by adding 1 μM $AgNO_3$ to the solution containing 60 μM H_2O_2, and a newly formed absorbance peak at 550 nm was observed in the UV-Vis spectra. The results of TEM (Figure S4) supported that the resulting AuNPs are well-dispersed with average diameter (38 ± 4 nm). The control experiments showed that $NaNO_3$ (anionic control) can't assist the H_2O_2-mediated AuNPs generation and the absence of H_2O_2

or $HAuCl_4$ induces negligible color change. All these results revealed that Ag^+ actually played a key role in assisting the formation of well-dispersed AuNPs at low concentration of H_2O_2. Furthermore, the time-dependent $A_{550/650}$ ratio variations were also investigated (Figure S5). The $A_{550/650}$ ratio changed from about 1 to 2 within 10 min after the reduction reaction starts by addition of H_2O_2 solution into $AgNO_3/HAuCl_4$ mixture, indicating that the Ag^+-assisted AuNPs generation is quick. Thus, both of the UV-Vis spectra and photographs in the following experiments were recorded at 15 min after addition of reductant H_2O_2.

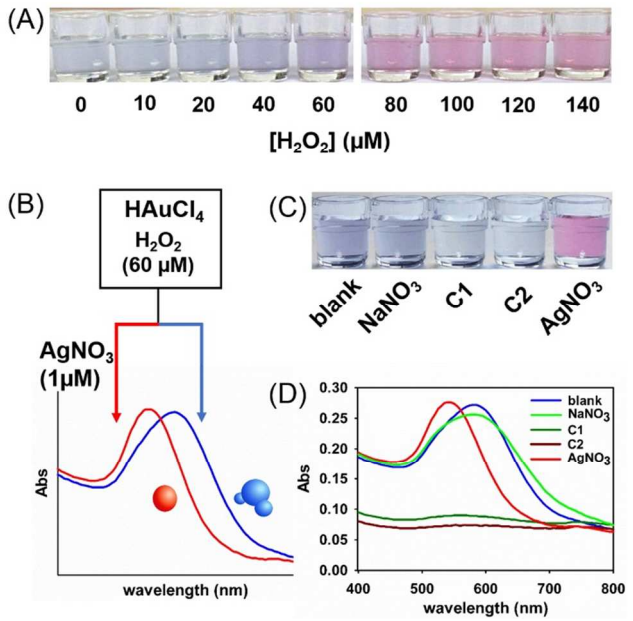

Figure 1. (A) Generation of nanoparticle solutions with different colors depending on the concentration of H_2O_2. (B) The scheme of Ag^+-assisting AuNPs growth. The red well-dispersed AuNPs solution was generated by adding Ag^+ (1 μM) to the solution containing H_2O_2 (60 μM) and $HAuCl_4$ (0.1 mM) in MES buffer. (C) Different color and (D) UV–Vis spectra of AuNPs solutions obtained under different reaction condition: $AgNO_3$: $AgNO_3$ (1 μM), H_2O_2 (60 μM) and $HAuCl_4$ (0.1 mM); Blank: the control without $AgNO_3$; C1: the control without H_2O_2; C2: the control without $HAuCl_4$; $NaNO_3$: the control using $NaNO_3$ (1 μM) instead of $AgNO_3$.

Furthermore, for a deeper insight into the influence of Ag^+ on AuNPs production, AuNPs was prepared with different concentrations of Ag^+ (0 ~ 5 μM) and H_2O_2 (60 μM), and an unexpected phenomenon was observed. As shown in Figure 2A and 2B, blue solution was obtained without Ag^+, and the color of solutions retains blue with increasing the concentration of Ag^+ from 0 to 0.1 μM. However, when the concentration of Ag^+ surpasses the threshold A (0.1 μM), the color of solutions dramatically changed from blue to red, and accordingly the $A_{550/650}$ value switched from $A_{550/650} < 2$ to $A_{550/650} > 2$. The concentration threshold A can be seen as a chemical switch that turned on the colorimetric signal (from blue to red). Furthermore, the color of solutions would remain red in the concentration interval of Ag^+ between 0.1 μM and 1 μM. Nevertheless, there was also a sudden color change from red to light blue once the concentration of Ag^+ exceeded threshold B (1 μM), which was consistent with the value $A_{550/650}$ dropped from the value > 2 to the value < 2. Thus threshold B was regarded as the other chemical switch to turn off the colorimetric signal. The color would retain light blue with further increase of Ag^+ concentration. All the detailed absorbance spectra of AuNPs prepared at different silver concentrations are shown in Figure S6. If the blue ($A_{550/650} < 2$) and red AuNPs solutions ($A_{550/650} > 2$) were defined as colorimetric output signal OFF and ON, respectively, this Ag^+ concentration-dependent colorimetric signal profile can be outputted in a format of OFF-ON-OFF, which was similar to the square wave in electrics. Thus, we name this colorimetric signal profile as the chemically colorimetric square wave, and the Ag^+ concentration-dependent chemical colorimetric square wave (Ag^+-CCSW) can be constructed based on Ag^+-assisted AuNPs generation.

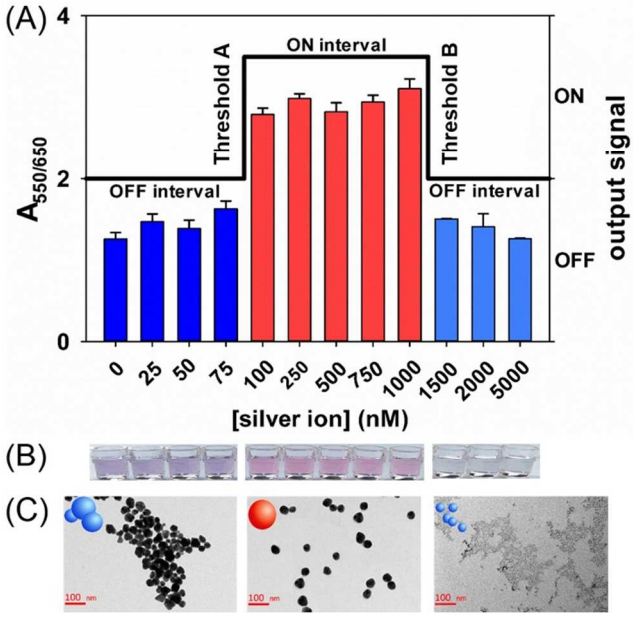

Figure 2. The construction of Ag^+ concentration-dependent chemical colorimetric square wave (Ag^+-CCSW). (A) The presentation of the Ag^+-CCSW: the ratio $A_{550/650}$ and the corresponding colorimetric output signal of AuNPs solutions versus different Ag^+ concentrations. $A_{550/650} > 2$ and $A_{550/650} < 2$ stands for the output signal ON and OFF, respectively. (B) The color change (blue-red-blue) of AuNPs solution with different concentrations of Ag^+. (C) The images of TEM represent the state of AuNPs obtained with different concentrations of Ag^+ (0.075 μM, 1 μM and 5 μM, respectively).

According to the Ag^+-CCSW, the examined Ag^+ concentration range from 0 to 5 μM can be divided into three intervals: the first OFF interval (0 to 0.1 μM), the ON interval (0.1 to 1 μM), and the second OFF interval (1 to 5 μM). TEM images were applied to further investigate the influence of different concentration intervals of Ag^+ on morphology and state of AuNPs. As depicted in Figure 2C, the cluster-like AuNPs aggregates were produced with 0.075 μM Ag^+ (the first OFF interval) but well-dispersed AuNPs were formed with an average diameter of 38 ± 4 nm at 1 μM Ag^+ (the ON interval). Nonetheless, the remarkably decreased amount of AuNPs in heavily aggregated state and numerous unformed gold nuclei were observed with 5 μM Ag^+ (the second interval OFF). DLS analysis (Figure S7) indicated that the first OFF interval of Ag^+ concentration (0.075 μM) yields the AuNPs aggregation with a large size and wide size distribution. However, smaller size and narrower size distribution was observed in nanoparticles solution grown with Ag^+ concentration in ON interval (1 μM). Relative weak DLS signal was observed in second OFF interval (5 μM Ag^+), implying the existence of unformed gold nuclei. All the results of the DLS experiments were consistent with TEM images. Moreover, EDX analysis of AuNPs grown with different concentrations of $AgNO_3$ was also performed. The EDX spectra (Figure S8) showed the nanoparticles were composed of Au element (Ag signal was invisible, while the Cu and C signal came from the copper grid), which confirmed that the nanoparticles obtained were AuNPs, rather than AgNPs.

This Ag^+ concentration-dependent AuNPs morphology change might be due to that certain Ag^+ concentration is required to promote the shape control of AuNPs to form dispersed quasi-spherical AuNPs. Under the condition with proper concentration of Ag^+, the under potential deposition (UPD) of Ag^+ on the surface of AuNPs to yield Ag coverage and stabilize a higher energy surface facets which are the reactive toward AuNPs aggregation[39], but more Ag^+ would greatly slow down the growth of gold nanostructures probably due to two reasons: the silver ion-catalyzed the decomposition of H_2O_2 to diminish the concentration of H_2O_2[40] and the inhibition of gold reduction and deposition on the gold nucleic because of excessive UPD of Ag^+ ion[41]. Moreover, the dynamic change of colorimetric signal was measured for monitoring the AuNPs growth process. As shown in Figure S9, the $A_{550/650}$ value changed within 10 min after H_2O_2 addition to initiate reaction, indicating the quick process of AuNPs generation. Only the Ag^+ concentration within the ON interval resulted in $A_{550/650} > 2$, consistent with the results of the photographs.

Since Ag^+ can be employed to assist the growth of AuNPs and further construct the CCSW, it is interesting to examine whether the other metal ions have the same effect on the generation of AuNPs. Therefore, colorimetric response of this AuNPs growth system was investigated in the presence of various metal ions, including Ag^+, K^+, Mg^{2+}, Pb^{2+}, Pd^{2+}, Sr^{2+}, Cu^{2+}, Mn^{2+}, Ni^{2+}, Cd^{2+}, Hg^{2+}, Co^{2+}, Fe^{2+}, Fe^{3+}, Cr^{3+}. Ag^+ was examined at 1 μM, while other metal ions were tested at 1 μM (Figure S10) and 20 μM (Figure 3), respectively. As exhibited in Figure 3 and Figure S10, only Ag^+ can induce a remarkable red AuNPs solution and significantly increase the ratio $A_{550/650}$ to exceed 2 in the presence of 60 μM H_2O_2, while other metal ions showed negligible effect (blue color or colorless and the $A_{550/650} < 2$) compared with the blank, probably resulting from that other metal ions had no positive effect (*e.g.* K^+ and Mg^{2+}), or even negative effect (*e.g.* Mn^{2+}, Fe^{2+} and Fe^{3+}) on the formation of AuNPs.

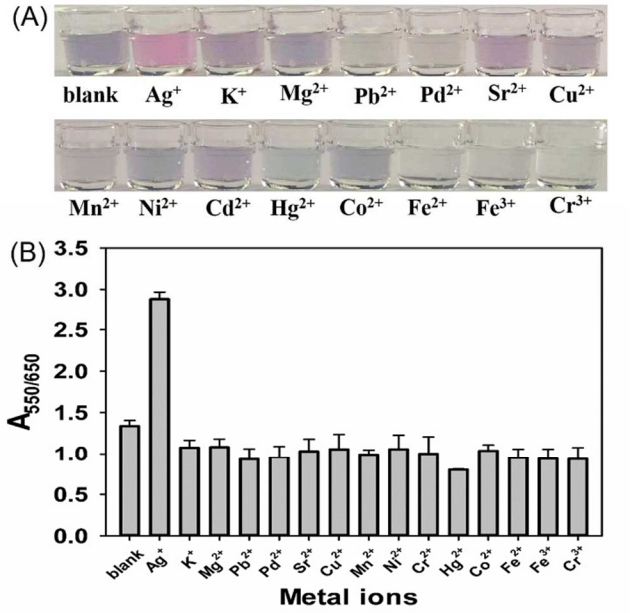

Figure 3. The selectivity of metal ions for assisting the growth of AuNPs and constructing the CCSW. (A) Different color and (B) the absorption ratio ($A_{550/650}$) of AuNPs solution obtained with 60 μM H_2O_2 and in the presence of 1 μM Ag^+ and 20 μM other metal ions, respectively.

On one hand, some metal ions catalyze the decomposition of H_2O_2 at different rates, which may result in different amount of H_2O_2 in the solutions[40c]; on the other hand, many metal ions cannot promote disproportionation of Au (I) complexes[42] and have different UPD on AuNPs [41b, 43]. These reasons may account for the phenomenon that the other metal ions had no obvious effect upon the AuNPs generation. The ratio $A_{550/650}$ showed that other metal ions couldn't cause obvious response change. These results indicated that the selectivity of metal ion assistant AuNPs generation for Ag^+ was excellent.

3.3 Establishment of the pH-CCSW

The status of AuNPs could be varied by altering the pH value of the reaction solution[44], thus it is important to investigate the formation of AuNPs with Ag^+ at different pH values. The experiments were performed in the mixture containing H_2O_2 (60 μM), Ag^+ (1 μM), $HAuCl_4$ (0.1 mM) and MES buffer with varying pH values (3.2 ~ 8.5). As shown in Figure 4, light blue solution was obtained with pH 3.2 MES buffer. Furthermore, the solution would maintain light blue ($A_{550/650} < 2$) with increasing the pH value of solution gradually. However, when the pH value increased to the threshold A' (pH 5.5), the solution presented a sudden color change from light blue to red. The solution color retained red ($A_{550/650} > 2$) in the pH interval from 5.5 to 6.5. Nevertheless, there was also an abrupt color change of solution from red to blue at pH 6.5, indicating a switch (threshold B', pH 6.5) to turn off the colorimetric signal. Hereafter, the color would keep blue ($A_{550/650} < 2$) with increase of pH value. All the detailed absorbance spectra of AuNPs prepared at

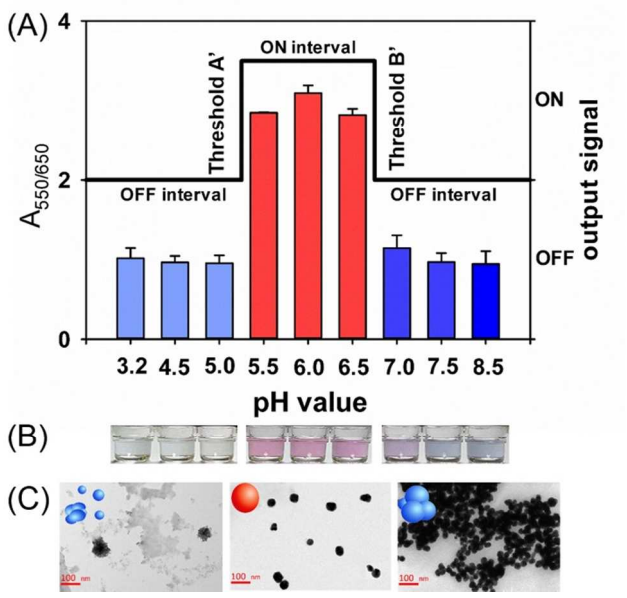

Figure 4. The construction of pH dependent chemical colorimetric square wave (pH-CCSW). (A) The presentation of the pH-CCSW: the ratio $A_{550/650}$ and the corresponding colorimetric output signal of AuNPs solutions versus different pH values. (B) The color change (blue-red-blue) of AuNPs solutions with different pH values. (C) The TEM images of AuNPs formed at pH 3.2, pH 6.5 and pH 8.5, respectively.

different pH values are shown in Figure S11. Furthermore, the dynamic monitoring of $A_{550/650}$ ratio change implied that the AuNPs growth in different pH values all finished in 10 min (Figure S12). Therefore, in response to pH value increased, the color of solutions changed in a format of blue-red-blue, which was similar to the afore-mentioned Ag^+-CCSW. Accordingly, using the same approach, the pH-dependent chemical colorimetric square wave (pH-CCSW) was successfully constructed. In this pH-CCSW, the pH-dependent output signal was displayed as OFF-ON-OFF profiles and the examined pH range can be divided into three pH intervals: the first

OFF interval with pH less than 5.5, the ON interval with pH ranging from 5.5 to 6.5, and the second OFF interval with pH above 6.5. Two threshold pH values, 5.5 and 6.5, play the roles as the turn-on switch and turn-off switch for colorimetric signal, respectively.

The TEM and DLS experiments were performed to further investigate the AuNPs obtained. Figure 4C shows the TEM images of the nanoparticles grown at different pH values. Numerous unformed gold nuclei and some aggregated clusters were observed at pH 3.2 (the first interval OFF). Conversely, well-dispersed AuNPs with an average diameter of 38 ± 5 nm were formed with pH 6.5 (the ON interval). Nonetheless, the AuNPs composed by a large number of particles with an average diameter of 31 ± 9 nm were obtained at pH 8.5 (the second OFF interval). In accordance with the TEM results, DLS analysis (Figure S13) revealed that the ON interval of pH caused significantly smaller size and narrower size distribution of AuNPs in comparison with the second OFF interval of pH, and only ultra-small substances was obtained at the first OFF interval of pH. Therefore, these results demonstrated that the growth of nanoparticles was a tunable phenomenon with state changes by changing the pH of solutions.

The effect of pH on the AuNPs generation might result from the different properties of gold complexes and H_2O_2 in solutions with different pH values. Depending on the pH values of solutions, $AuCl_4^-$ ions (pH 3.3) are hydrolyzed into different types of auric precursor ions with different reactive activity in the following sequence: $AuCl_4^-$ > $AuCl_3(OH)^-$ (pH 6.2) > $AuCl_2(OH)_2^-$ (pH 7.1) > $AuCl(OH)_3^-$ (pH 8.1) > $Au(OH)_4^-$ (pH 12.9)[42, 43]. In addition, the oxidation of H_2O_2 is weakened with increasing of pH value, but reduction ability is enhanced with accelerating the decomposition rate of H_2O_2[41]. Both of these reasons may lead to the formation of different states AuNPs. The coupling effect of these factors influences the formation of different states AuNPs. The poor productivity of AuNPs at first OFF interval probably relies on the weak reduction ability of H_2O_2 at low pH; the proper reduction ability at ON interval of pH causes the well-dispersed AuNPs; the relative high pH at second OFF interval induces the week reactive activity of gold ion complex and more depletion of H_2O_2 by accelerating the decomposition, resulting in AuNPs aggregation.

3.4 Logic gates based on integrations of the CCSW

The above results demonstrate the growth of AuNPs via reduction by H_2O_2 is highly dependent on the concentration of Ag^+ and the solution pH value. The key point in the CCSW is to control the aggregation of AuNPs to yield red and blue solution dependent on regulation of the concentration of Ag^+ and pH, respectively. Changing the concentration of Ag^+ and pH from the OFF interval to ON interval will cause the switch on of colorimetric signal, which sets the output state as 1. Therefore, it can be expected to build logic gate by employing the effects of Ag^+ and pH on forming AuNPs. The AND, OR and INHIBIT logic gates were constructed by means of integrating the Ag^+-CCSW and pH-CCSW mentioned above. In the AND gate, there was an output 1 only if both of the inputs were held at 1. The AuNPs growth mixture containing H_2O_2 (60 μM) and $HAuCl_4$ (0.1 mM) in MES buffer (pH 8.5) worked as the initial condition. In order to implement the AND gate, Ag^+ and H^+ were defined as inputs and the color of AuNPs solution as output. For the inputs, the addition of Ag^+ and acid MES buffer (H^+, pH 3.2) was defined as 1, respectively, otherwise defined as 0. For the output, 1 represented red solution with $A_{550/650} > 2$, while 0 stood for the blue solution with $A_{550/650} < 2$. In the (0/0) state, blue AuNPs solution (output = 0) was displayed, since both of the Ag^+ concentration and pH were located in the OFF intervals of two CCSWs as shown in the table of Figure 5. In the (1/0) state, Ag^+ was added and its final concentration was 1 μM, which was located at the ON interval of the Ag^+-CCSW, but purple solution was still obtained (output = 0) because the pH was at the OFF interval of the pH-CCSW. In the (0/1) state, the acid MES buffer (pH 3.2) was added to adjust pH from 8.5 to 6.5, which lies in the ON interval of the pH-CCSW, and blue solution was also obtained (output = 0) because of the concentration of Ag^+ settled in the OFF interval. However, when both Ag^+ and H^+ (acid MES buffer) were introduced and they were both settled in the ON interval of two kinds of CCSW, that is, in the (1/1) state, red solution (output = 1) would be observed. Therefore, the output of logic gate is 1 only when the inputs are (1/1), and the outputs of other three inputs (0/0), (1/0), (0/1) are 0, which descripts this is a typical AND logic gate.

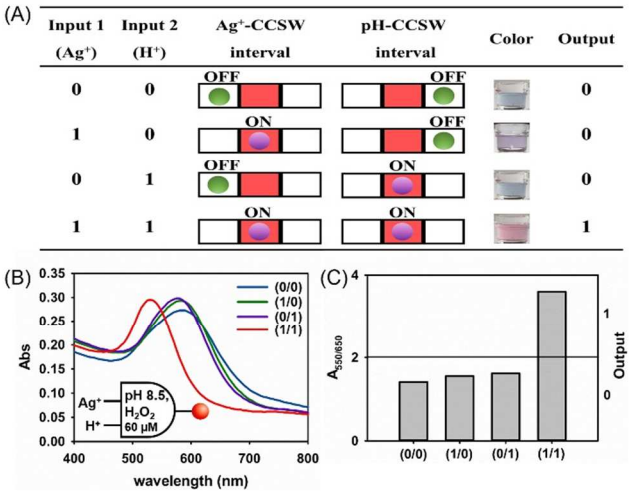

Figure 5. The CCSW-based AND logic gate: (A) The truth table of the AND gate and the corresponding intervals of the Ag^+-CCSW and pH-CCSW. (B) The corresponding UV-Vis absorption responses and (C) bar chart of the outputs of the AND logic gate. For the bar chart, the absorbance ratio value $A_{550/650}$ of 2 was marked as the output signal threshold.

Furthermore, the INHIBIT gate could be established via integrating two CCSWs. The INHIBIT gate demonstrated noncommutative behavior, which meant that one input had the power to disable the whole system. As shown in Figure 6, the initial condition is that the mixture contains H_2O_2 (60 μM) and $HAuCl_4$ (0.1 mM) in MES

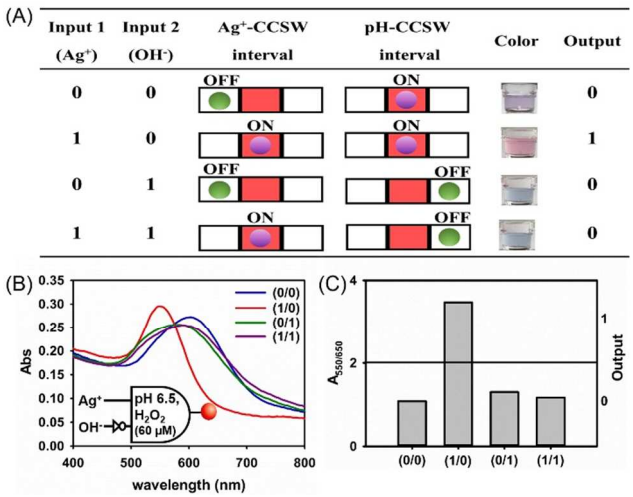

Figure 6. The CCSW-based INHIBIT logic gate: (A) The truth table of the INHIBIT gate and the corresponding intervals of the Ag^+-CCSW and pH-CCSW.

(B) Absorbance features and (C) bar chart of the absorbance outputs of the INHIBIT gate.

buffer (pH 6.5). In the INHIBIT gate, Ag^+ and OH^- were defined as inputs and the color of solution defined as output. For the inputs, the addition of Ag^+ and NaOH (OH^-) was defined as 1, respectively, otherwise defined as 0. For the output, 1 represented red solution with $A_{550/650} > 2$, while 0 stood for the blue solution with $A_{550/650} < 2$. In the (0/0) state, blue AuNPs solution (output = 0) appeared, however, in the (1/0) state, the addition of 1 μM Ag^+ induced red solution (output = 1) because the concentration of Ag^+ and pH were both in the ON intervals of two CCSW. Nevertheless, in the (0/1) state, NaOH was added to adjust the pH of solution from pH 6.5 to pH 8.5 and pH would settle in the OFF interval of the pH-CCSW, which leads to blue solution (output = 0). When both Ag^+ and OH^- were introduced and the concentration of Ag^+ and pH value were settled in the interval ON and OFF of the two CCSWs, respectively, i.e. in the (1/1) state, blue solution (output = 0) was observed. Therefore, the output of logic gate is 1 only when the inputs are (1/0), and the outputs of other three inputs (0/0), (0/1), (1/1) are 0, which is the typical representation of INHIBIT gate.

In addition, the OR gate was built through taking advantage of the Ag^+-CCSW and H_2O_2-mediated AuNPs generation. In this OR logic gate (Figure 7), Ag^+ and H_2O_2 were defined as inputs and the color of solution after reduction reaction defined as output. For the inputs, the addition of Ag^+ and H_2O_2 was defined as 1, respectively, otherwise the inputs were defined as 0. For the output, 1 represented red solution with $A_{550/650} > 2$, while 0 stood for the blue solution with $A_{550/650} < 2$. The initial reaction mixture was comprised of H_2O_2 (60 μM) and $HAuCl_4$ (0.1 mM) in MES buffer (pH 6.5). With no input

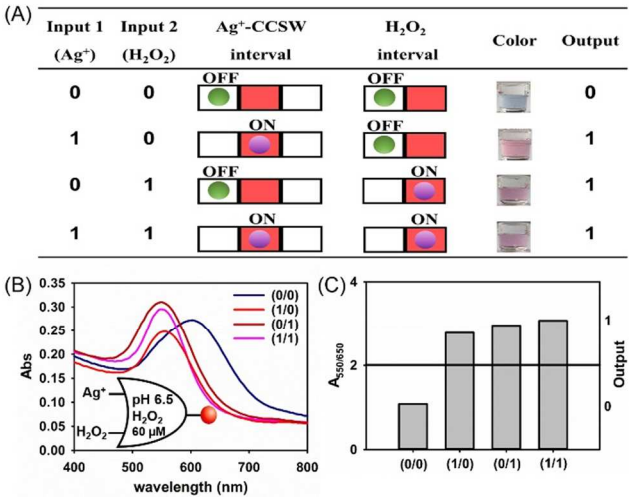

Figure 7. The CCSW-based OR logic gate: (A) The truth table corresponding to the OR gate taking advantage of the Ag^+-CCSW and H_2O_2-mediated AuNPs generation. (B) Absorbance features and (C) bar chart of the absorbance outputs of the OR gate.

(0/0), the initial reaction mixture (output = 0) caused the blue solution. However, with Ag^+ input alone (1/0), the final concentration of Ag^+ was 1 μM (located in the ON interval of the Ag^+-CCSW), and red solution was obtained (output = 1). For H_2O_2 input alone (0/1), additional H_2O_2 was introduced to increase the concentration of H_2O_2 to 80 μM, which was the critical concentration of H_2O_2 to form red AuNPs solution (output = 1). Moreover, with two inputs together, the concentration of Ag^+ was located in the ON interval (1 μM) of the Ag^+-CCSW and the concentration of H_2O_2 was 80 μM, resulting in a red solution (output = 1). Therefore, only the input (0/0) would generate blue solution (output = 0), while the outputs of other inputs (1/0), (0/1), (1/1) are 1, which is a typical OR gate. Therefore, through the integrations of these CCSWs, the AND, INHIBIT, OR logic gates were successfully constructed. These AuNPs logic gates are based on the tunable growth of AuNPs, which are simple, reliable and economic without complicated AuNPs modification and triggered crosslinking.

4. Conclusions

In summary, a novel, label-free and simple AuNPs-based chemical colorimetric square wave device (CCSW) with two switches have been successfully constructed based on the tunable plasmonic changes during the generation of AuNPs. Two instances of the CCSW dependent on Ag^+ concentration and pH were established according to the special effects of the Ag^+ concentration and pH value on the AuNPs growth, respectively. Furthermore, the Ag^+-CCSW possesses excellent selectivity, which can be used to distinguish Ag^+ from other metal ions. What's more, we established the AND, INHIBIT and OR logic gates via rational integration of these two CCSWs. This novel AuNPs based CCSW possessed some fascinating features: 1) a new concept of the CCSW was proposed based on the discontinuous plasmonic change during the generation process of AuNPs; 2) The CCSW was easy to construct because of the simple and rapid procedures, as well as mild conditions for AuNPs formation; 3) Unlike conventional AuNPs-based logic gates depending on crosslinking or non-crosslinking aggregation, these CCSW-based logic gates relied on the controllable growth of AuNPs, which widened the application of colorimetric logic gates; Moreover, more CCSWs and relative logic gates could be developed through further exploring the conditions regulating the growth of AuNPs or other plasmonic metal nanoparticles. This concept opened up a new possibility for sensing when chemistry of crystal growth was merged with the outstanding physical properties of nano-sensors. Therefore, further investigation on novel CCSWs may have potential value and broad applications in analytical and material sciences.

Acknowledgements

This work was financially supported by the National Natural Science Foundation of China (Nos. 21222507, 21175036, 21235002, and 21190044), the National Basic Research Program of China (973 Program, No. 2011CB911002), the Foundation for Innovative Research Groups of NSFC (Grant 21221003), and the Ph.D. Programs Foundation of the Ministry of Education of China (No.20120161110025).

Notes and references

State Key Laboratory of Chemo/Biosensing and Chemometrics, College of Chemistry and Chemical Engineering, Hunan University, Changsha, 410082, P. R. China. Fax: +86-731-88821848; Tel: +86-731-88821626;
E-mail:niezhou.hnu@gmail.com (Z. Nie)

† Electronic Supplementary Information (ESI) available: Figure. S1-S13.
See DOI: 10.1039/b000000x/

1 M. Hu, J. Chen, Z.-Y. Li, L. Au, G. V. Hartland, X. Li, M. Marquez and Y. Xia, *Chem. Soc. Rev.*, 2006, **35**, 1084-1094.
2 S. V. Boriskina and B. M. Reinhard, *Nanoscale*, 2012, **4**, 76-90.
3 R. A. Reynolds, C. A. Mirkin and R. L. Letsinger, *J. Am. Chem. Soc.*, 2000, **122**, 3795-3796.
4 Y. F. Li and C. Chen, *Small*, 2011, **7**, 2965-2980.

5 P. K. Jain, K. S. Lee, I. H. El-Sayed and M. A. El-Sayed, *J. Phys. Chem. B*, 2006, **110**, 7238-7248.
6 C.-W. Lien, Y.-C. Chen, H.-T. Chang and C.-C. Huang, *Nanoscale*, 2013, **5**, 8227-8234.
7 Y. Ofir, B. Samanta and V. M. Rotello, *Chem. Soc. Rev.*, 2008, **37**, 1814-1825.
8 R. Elghanian, J. J. Storhoff, R. C. Mucic, R. L. Letsinger and C. A. Mirkin, *Science*, 1997, **277**, 1078-1081.
9 N. L. Rosi and C. A. Mirkin, *Chem. Rev.*, 2005, **105**, 1547-1562.
10 B. Kowalczyk, I. Lagzi and B. A. Grzybowski, *Nanoscale*, 2010, **2**, 2366-2369.
11 D. Liu, Z. Wang and X. Jiang, *Nanoscale*, 2011, **3**, 1421-1433.
12 J. Wang and X. Qu, *Nanoscale*, 2013, **5**, 3589-3600.
13 J. Du, L. Jiang, Q. Shao, X. Liu, R. S. Marks, J. Ma and X. Chen, *Small*, 2013, **9**, 1467-1481.
14 F. Xia, X. Zuo, R. Yang, Y. Xiao, D. Kang, A. Vallée-Bélisle, X. Gong, J. D. Yuen, B. B. Hsu and A. J. Heeger, *PNAS*, 2010, **107**, 10837-10841.
15 Ž. Krpetić, L. Guerrini, I. A. Larmour, J. Reglinski, K. Faulds and D. Graham, *Small*, 2012, **8**, 707-714.
16 Y.-C. Yeh, B. Creran and V. M. Rotello, *Nanoscale*, 2012, **4**, 1871-1880.
17 M. R. Hartman, R. C. Ruiz, S. Hamada, C. Xu, K. G. Yancey, Y. Yu, W. Han and D. Luo, *Nanoscale*, 2013, **5**, 10141-10154.
18 H. Zhang, F. Li, B. Dever, X.-F. Li and X. C. Le, *Chem. Rev.*, 2012, **113**, 2812-2841.
19 R. Huang, R. P. Carney, F. Stellacci and B. L. Lau, *Nanoscale*, 2013, **5**, 6928-6935.
20 A. Leifert, Y. Pan-Bartnek, U. Simon and W. Jahnen-Dechent, *Nanoscale*, 2013, **5**, 6224-6242.
21 H. Jans and Q. Huo, *Chem. Soc. Rev.*, 2012, **41**, 2849-2866.
22 H. Wang, L. Zheng, C. Peng, R. Guo, M. Shen, X. Shi and G. Zhang, *Biomaterials*, 2011, **32**, 2979-2988.
23 N. M. Schaeublin, L. K. Braydich-Stolle, A. M. Schrand, J. M. Miller, J. Hutchison, J. J. Schlager and S. M. Hussain, *Nanoscale*, 2011, **3**, 410-420.
24 R. de La Rica and M. M. Stevens, *Nat. Nanotechnol.*, 2012, **7**, 821-824.
25 L. Rodríguez-Lorenzo, R. de La Rica, R. A. Álvarez-Puebla, L. M. Liz-Marzán and M. M. Stevens, *Nat. Mater.*, 2012, **11**, 604-607.
26 X. Liu, S. Zhang, P. Tan, J. Zhou, Y. Huang, Z. Nie and S. Yao, *Chem. Commun.*, 2013, **49**, 1856-1858.
27 X. Zhu, H. Xu, X. Gao, X. Li, Q. Liu, Z. Lin, B. Qiu and G. Chen, *Chem. Commun.*, 2011, **47**, 9080-9082.
28 K. Ariga, H. Ito, J. P. Hill and H. Tsukube, *Chem. Soc. Rev.*, 2012, **41**, 5800-5835.
29 I. Willner, B. Shlyahovsky, M. Zayats and B. Willner, *Chem. Soc. Rev.*, 2008, **37**, 1153-1165.
30 S. Bi, Y. Yan, S. Hao and S. Zhang, *Angew. Chem.*, 2010, **122**, 4540-4544.
31 J. Du, S. Yin, L. Jiang, B. Ma and X. Chen, *Chem. Commun.*, 2013, **49**, 4196-4198
32 P. Zhan, J. Wang, Z. G. Wang and B. Ding, *Small*, 2014, **10**, 399-406.
33 Q. Jiang, Z. G. Wang and B. Ding, *Small*, 2013, **9**, 1016-1020.
34 D. Liu, W. Chen, K. Sun, K. Deng, W. Zhang, Z. Wang and X. Jiang, *Angew. Chem. Int. Ed.*, 2011, **50**, 4103-4107.
35 X. Xu, J. Zhang, F. Yang and X. Yang, *Chem. Commun.*, 2011, **47**, 9435-9437.
36 P. CooperáStevenson, *Spec. Discuss. Faraday Soc.*, 1951, **11**, 55-75.
37 M.-C. Daniel and D. Astruc, *Chem. Rev.*, 2004, **104**, 293-346.
38 J. Liu and Y. Lu, *J. Am. Chem. Soc.*, 2003, **125**, 6642-6643.
39 (a) C. J. Orendorff and C. J. Murphy, *J. Phys. Chem. B*, 2006, **110**, 3990-3994; (b) Y. Xianyu, J. Sun, Y. Li, Y. Tian, Z. Wang and X. Jiang, *Nanoscale*, 2013, **5**, 6303-6306; (c) M. L. Personick, M. R. Langille, J. Zhang and C. A. Mirkin, *Nano Lett.*, 2011, **11**, 3394-3398.
40 (a) M. Liu and P. Guyot-Sionnest, *J. Phys. Chem. B*, 2005, **109**, 22192-22200; (b) S.-S. Lin and M. D. Gurol, *Environ. Sci. Technol*, 1998, **32**, 1417-1423; (c) J. Weiss, *Transactions of the Faraday Society*, 1935, **31**, 1547-1557.
41 (a) A. K. Das and C. R. Raj, *J. Phys. Chem. C*, 2011, **115**, 21041-21046; (b) D. Kolb, M. Przasnyski and H. Gerischer, *J. Electroanal. Chem. Interfacial Electrochem.*, 1974, **54**, 25-38; (c) M. R. Deakin and O. Melroy, *J. Electroanal. Chem. Interfacial Electrochem.*, 1988, **239**, 321-331; (d) S. Szabó, *International Reviews in Physical Chemistry*, 1991, **10**, 207-248.
42 Swathirajan, S.; Bruckenstein, S. *Electrochim. Acta* 1983**,** ***28***, 865-877;
43 **(a)** D. Goia and E. Matijević, *Colloids Surf., A*, 1999, **146**, 139-152; (b) H. Xia, S. Bai, J. r. Hartmann and D. Wang, *Langmuir*, 2009, **26**, 3585-3589.

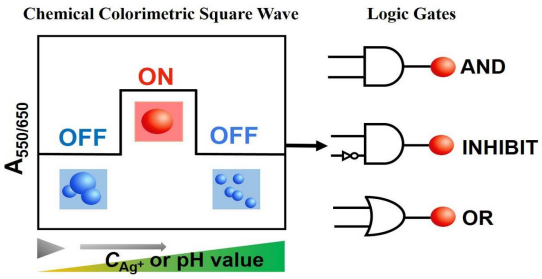

AuNPs-based chemical colorimetric square wave (CCSW) and logic gates were constructed based on the colorimetric signal change via the controllable growth of AuNPs.